

MEASURING THE ANISOTROPY IN THE CMB: CURRENT STATUS & FUTURE PROSPECTS

L.A. PAGE
Dept of Physics, Princeton University
Princeton, New Jersey
<http://physics.princeton.edu/~page>

Abstract.

The CMB is perhaps the cleanest cosmological observable. Given a cosmology model, the angular spectrum of the CMB can be computed to percent accuracy. On the observational side, as far as we know, there is little that stands in the way between an accurate measurement and a rigorous confrontation with theory. In this article, we review the state of the data and indicate future directions.

The data clearly show a rise in the angular spectrum to a peak of roughly $\delta T_l = (l(l+1)C_l/2\pi)^{1/2} \approx 85 \mu\text{K}$ at $l \approx 200$ and a fall at higher l . In particular, δT_l at $l = 400$ is significantly less than at $l = 200$. This is shown by a combined analysis of data sets and by the TOCO data alone.

In the simplest open models with $\Omega_m = 0.35$, one expects a peak in the angular spectrum near $l = 400$. For spatially flat models, a peak near $l = 200$ is indicated and thus this model is preferred by the data. The combination of this, along with the growing body of evidence that $\Omega_m \approx 0.3$, suggests a cosmological constant is required. Further evidence for a cosmological constant is provided by the height of the peak. This conclusion is independent of the supernovae data.

1. Introduction

These notes are from two talks given at the Newton Institute in July 1999. The goal was to assess the status of CMB anisotropy measurements and give some indication of what the future holds. Given the extraordinarily rapid development of this field, this article is sure to be outdated soon after it appears. The program included a section on interferometers and

the data therefrom by Anthony Lasenby, on the physics of the CMB by George Efstathiou, and on data analysis by Dick Bond so I shall not discuss those matters here. Anthony Lasenby also covered work on ESA's Planck satellite.

My talks are biased toward the experiments I know best. Some of the experiments which I will discuss, in particular the MAT experiments (a.k.a. TOCO97[59] and TOCO98[42]), were done by a collaboration between Mark Devlin's group at the University of Pennsylvania and the Princeton group.

It would be stunning if the currently popular model survived to be our favorite model of the universe in a few years. Recent panoramic assessments of cosmological data [1] [60] suggest the universe is made of $\Omega_b \approx 0.05$, $\Omega_{cdm} \approx 0.3$, & $\Omega_\Lambda \approx 0.65$ ¹. In other words, only 5% of the universe is made of something with which we are familiar.

There are three classes of observations that lead to the current picture. The supernovae data indicate that the universe is accelerating and thus need something like a cosmological constant to explain them. Secondly, the mass density, $\Omega_m = \Omega_b + \Omega_{cdm}$, as inferred from galactic velocities, cluster abundances, cluster x-ray luminosities, the S-Z effect in clusters, the cluster mass to light ratio, etc. is $\Omega_m \approx 0.35$. Thirdly, the CMB data suggest that the universe, within the context of adiabatic cold dark matter models, is spatially flat [1] [9]. The CMB data are improving rapidly. New data (TOCO97, TOCO98, CAT[2]), since [1], [9], strongly disfavor the nominal open spatial geometry models, and the case is getting tighter by the month [35]. We should point out that the position of the first peak does not *prove* the universe is spatially flat; there is enough wiggle room with the other parameters even within the limited context of adiabatic CDM models [34], but a spatially flat model is the simplest explanation when one assumes prior knowledge of other parameters such as H_0 .

2. The temperature of the CMB

In 1990 John Mather and colleagues [39], using the Far infrared Spectrophotometer (FIRAS) aboard the COBE satellite, showed that the CMB is a blackbody emitter over the frequency range of 70 to 630 GHz. It is perhaps the best characterized blackbody. A recent analysis [40] gives the temperature as $T = 2.725 \pm 0.002$ K (95% confidence). The error, 2 mK, is entirely systematic and so it is difficult to assign a precise confidence limit. The statistical error is of order $7 \mu\text{K}$. This measurement was quickly followed by the UBC rocket experiment [31] which found $T = 2.736 \pm 0.017$ K (1σ).

¹The b subscript stands for baryons, cdm for cold dark matter, and Λ for a cosmological constant type term.

At frequencies greater than 90 GHz, the FIRAS measurement will not be bettered without another satellite. At lower frequencies, the measurements are less precise and there is plenty of room for improvement. The best long wavelength measurement is by Staggs et al. [54] at 11 GHz. They find $T = 2.730 \pm 0.014$ K. Deviations from a pure thermal spectrum are expected to show up near a few GHz. In addition, we know the universe was reionized at $z \approx 5$, so there should be remnant free-free emission, also at a few GHz. Unfortunately, near these frequencies, our Galaxy emits about 2 K making a 0.01% determination of the CMB temperature difficult, to say the least. Our picture of the spectrum of the CMB will not be complete until the long wavelength part of the spectrum is known though only a few groups are seriously considering these tough experiments.

3. The unbiased anisotropy spectrum

Figure 1 shows all the anisotropy data that has at least made it into preprint form (as of this writing, Oct. 99, all of it has been accepted for publication). Many of the data points have not been confirmed or are essentially unconfirmable; others have large calibration errors; some data sets comprise sets of correlated points; still others have foreground contamination. Despite this, the trend is clear. From the Sachs-Wolfe plateau discovered by COME/DMR [53] there is a rise to an amplitude of $\delta T_l \approx 85 \mu\text{K}$ at $l \approx 200$ and a fall after that.

It is worth reviewing what sort of systematic checks we have between different experiments. At both large and small angular scales, the spectrum of the anisotropy is seen to be thermal. Also, at the largest angular scales, there is a clear correlation between DMR at 53 GHz and the FIRS data at 180 GHz [28]. In this analysis, the dust contribution to FIRS was subtracted though inclusion of it did not significantly alter the results: the dust is not correlated with the CMB. At smaller angular scales, SK at 35 GHz [43] saw the same signal as did the MSAM experiment at 200 GHz. In an analysis tour de force, Fixsen et al. [27] show that the COBE/FIRAS instrument—remember FIRAS is an absolute measurement—sees the same anisotropy as the COBE/DMR instrument which is a differential microwave radiometer. A plot of the cross correlation is consistent with a thermal spectrum from 90 to 300 GHz.

Outside of the above measurements, teams have not confirmed each others' findings. The reason is that it is difficult to match scan strategies from different instruments. This is one of the reasons that maps are desired. There are preliminary indications that the SK and QMAP maps agree [22] as do the maps from two seasons of PYTHON [13].

Figure 2 show all the data from Figure 1 binned into ten l -space bins.

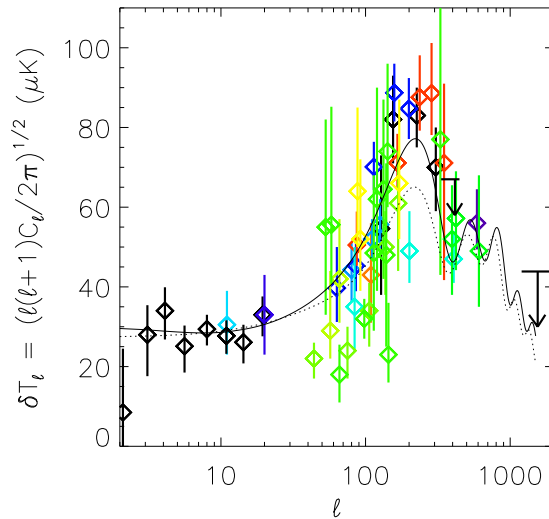


Figure 1. Unbiased sampling of data. The solid line on top is a model from Wang *et al.* (1999) with $\Omega_b = 0.05$, $\Omega_{cdm} = 0.3$, $\Omega_\Lambda = 0.65$, and $h = 0.65$. The dotted curve is the “standard cold dark matter” model, which is inconsistent with many non-CMB observations, with $\Omega_b = 0.05$, $\Omega_{cdm} = 0.95$, $\Omega_\Lambda = 0.0$, and $h = 0.5$. For the PYTHON 5 data we use the data from K. Coble’s thesis (Coble 1999) rather than those from the paper.

The plot is remarkable and gives us faith in the hot big bang model. The rise of the angular spectrum and the location of the peak for a spatially flat universe were predicted well in advance of the measurements. It is also satisfying that these data have shown that a number of alternative models simply do not work. For instance, large classes of isocurvature models do not fit the data (but by no means is the isocurvature mechanism excluded), simple open models do not fit the data [35], [25], and a broad class of defect models do not fit the data [45].

4. The observational setting & foreground emission

The CMB is a 2-D random field in temperature with variance of order $(115 \mu\text{K})^2$. If one could measure the anisotropy with sharp filters in l -space, one would find the *rms* variations for l between $2 < l < 40$ to be $54 \mu\text{K}$, between $40 < l < 400$ to be $88 \mu\text{K}$, and between $400 < l < 1500$ to be $53 \mu\text{K}$. So far, the data are consistent with a Gaussian temperature distribution.

Characterizing the anisotropy is challenging because one wishes to mea-

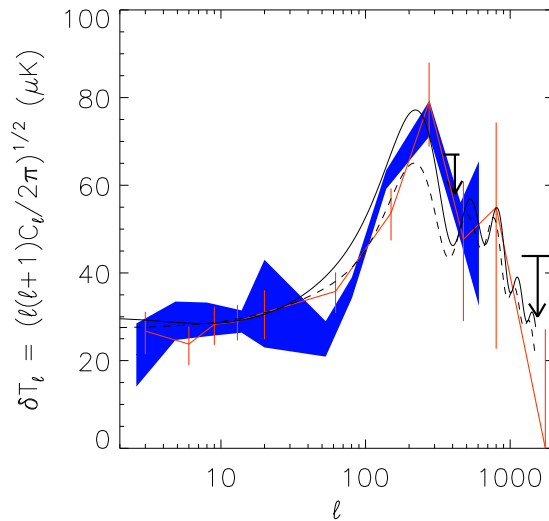


Figure 2. All the data from Figure 1 binned into ten logarithmically spaced bins. There is no accounting for calibration error, correlations, etc. The upper limits are at 95% confidence. The width of the blue swath is the statistical weight of the data that land in the corresponding bin. The orange line is a more sophisticated analysis by Bond *et al.* (1999) that uses a subset of the data in Figure 1.

sure accurately microkelvin variations from an experiment sitting on, or just above, a 300 K Earth. Nature, though, has been kind. The CMB is the brightest thing in the sky between 0.6 and 600 GHz; and fluctuations from emission from our Galaxy (for galactic latitudes $|b| > 20^\circ$) are smaller than the fluctuations intrinsic to the CMB [57], as shown in Figure 3. We do not yet know if we shall be so fortunate with the polarization, but low frequency measurements suggest this may be the case [17].

We may get a sense of the scale of the corrections for foreground emission from the SK data. SK observed near the North Celestial Pole at $b = 25^\circ$. The contribution to the original data set from foreground emission is 4% at 40 GHz [20]. It turns out the contamination was not due to free-free emission, Haslam-like synchrotron emission, or extra galactic sources, but rather was due to a component correlated with interstellar dust emission. The favorite current explanation is that this component is due to radiation by spinning dust grains [26]. This component was not expected when the experiment was conceived. In the QMAP experiment, the contamination at Ka (≈ 25 GHz) is $\approx 8\%$ [23]; no significant contribution to the Q band data was measured. Coble *et al.* [12], looking in the Southern Hemisphere at high Galactic latitudes, found effectively no contamination at 40 GHz.

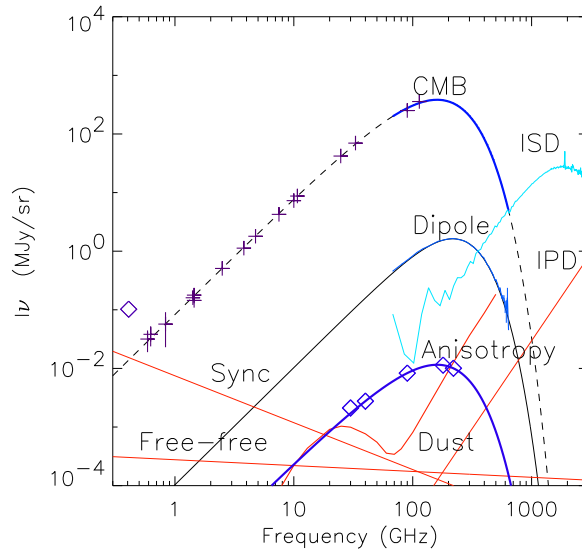


Figure 3. Plot of the CMB and the foreground emission at approximately the galactic latitude of the North Celestial Pole. For dust and synchrotron spectra, the fluctuating component has been plotted (de Oliveira-Costa *et al.* 1998). The flux levels of the free-free and dust emission have also been plotted. The corresponding l is about 20. At higher l , all these foregrounds have less fluctuation power. The FIRAS data (dust, dipole, and CMB spectra) are courtesy of Bill Reach.

5. Types of measurements

The scientific payoff from the CMB has motivated a large number of experiments; over twenty groups are trying to measure the anisotropy. The frequency coverage is large. The experiments and detector technologies are summarized in [3], [32], & [44].

Here we just note that there are three general classes of measurements. They are (1) beam switching or beam synthesis experiments, (2) direct mapping experiments, and (3) interferometers. By far the most data have come from the beam switching/synthesis method but this is certain to change soon.

The detectors of choice are high electron mobility transistor amplifiers (HEMTs [48], [49]) for frequencies below 100 GHz and bolometers for higher frequencies. The primary advantage of HEMTs is their ease of use and speed. A typical HEMT sensitivity is $0.5 \text{ mKs}^{1/2}$. The advantage of bolometers is their tremendous sensitivity, e.g. $< 0.1 \text{ mKs}^{1/2}$. The CMB anisotropy has also been detected with SIS mixers [36].

Over the past year, five new results from experiments have come out

of which I am aware. They are the IAC[18], CAT, QMAP, TOCO, and PYTHON 5. These data span from 30 to 150 GHz and from $l = 50$ to 400. They support the picture given in [9]. As an example of a beam switching experiment, I'll use TOCO; and as an example of a mapping experiment I'll use QMAP.

6. QMAP

The QMAP experiment is described in a trio of papers ([24], [33], & [20]). The purpose of QMAP, which was proposed before MAP, was to make a “true” map of the sky at 30 and 40 GHz. By true map we mean a map that is simply described by a temperature and temperature uncertainty per pixel. Ideally, the pixel to pixel covariance matrix is diagonal. For QMAP, this was not the case and the full covariance matrix was required. Maps that are reconstructed from beam switching measurements, for instance the SK[56], MSAM[37], MAX[62], and PYTHON 5[13] maps, are not true maps and cannot be analyzed as maps.

QMAP is a direct mapping experiment. The data stream is converted directly into a map and the covariance matrix is computed from the data. So far, only four experiments have directly mapped the CMB anisotropy (COBE/FIRAS, COBE/DMR, FIRS, and QMAP). QMAP, so far, has the highest S/N per pixel. We can look forward to the BOOMERanG [10] and MAXIMA [41] data which, with their tremendous detectors, should produce much higher sensitivity maps.

The key to making a map is to “connect each pixel with all the ones around it.” [55] [65]. In simplest terms, one wants to sit at a pixel and know the derivatives in each direction. QMAP accomplished this connectedness by observing above the North Celestial Pole and letting the sky rotate through the beam. The scan lines thus intersect at a variety of angles [24]. Maps that are reconstructed from temperature differences (e.g. from beam switching experiments) do not generally have this property because the differences are all done at constant elevation (SK is an exception; again the rotation around the North Celestial Pole was used.)

The QMAP power spectrum is given in Table 1. With the two flights, and six channels per flight a number of cross checks can be made. The data common to both flights and between channels within one flight are consistent. In a chi-by-eye, the QMAP map looks very similar to the reconstructed SK map in areas where they overlap [22].

The QMAP data are extremely clean. There is essentially no editing of spurious points etc. One simply takes the data, calibrates it, removes a slowly varying offset (this is done self-consistently in the map solution) and produces the map. It is the type of data set for which the analysis pipeline

Devlin, de Oliveira-Costa, Herbig, Miller, Netterfield, Page & Tegmark 1998
 Herbig, de Oliveira-Costa, Devlin, Miller, Netterfield, Page & Tegmark 1998
 de Oliveira-Costa, Devlin, Herbig, Miller, Netterfield, Page & Tegmark 1998

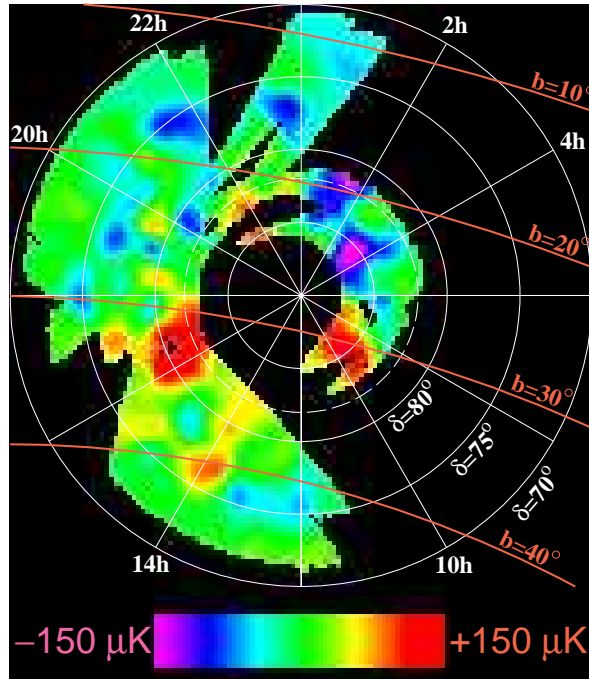


Figure 4. Results of two QMAP flights. There are multiple spots in the map with a signal to noise of 10 to 20. SK fills the region within $\delta = 82^\circ$ shown by the dashed line. This plot shows a Wiener filtered version of the raw map. This is what the anisotropy looks like at degree angular scales.

could have been written before the experiment.

7. MAT/TOCO

The MAT/TOCO experiment is a collaboration between Mark Devlin's group at Penn and the Princeton group. We took the QMAP gondola and optics, changed the cooling from liquid helium to a mechanical refrigerator, and mounted the telescope on a Nike Ajax radar trailer. For two seasons (Oct.-Dec. 1997 and Jun.-Dec. 1998) we observed from Cerro Toco near the

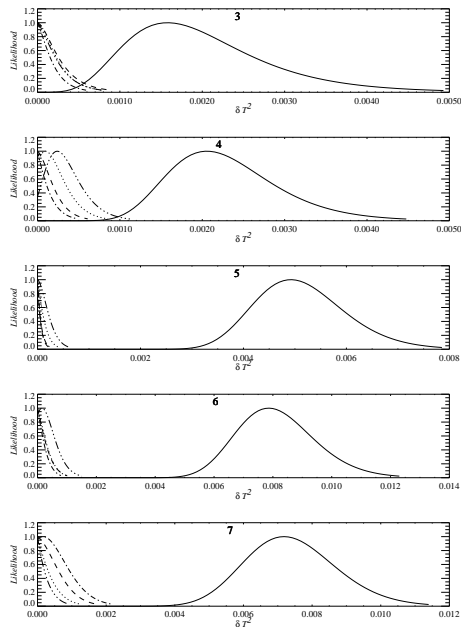


Figure 5. The likelihood of the data and the likelihood of the null combinations of the TOCO97 data set. The four null signals are data taken with the chopper scanning one way minus data with the chopper scanning the other, differences between subsequent 0.25 s segments, differences between subsequent 5 s segments, and the first half minus the second half of the campaign. From top to bottom, the panels correspond to $l = 63, 86, 114, 158, \& 199$ as given in Table 1.

ALMA site in the northern Chilean Andes.²

In the first season (TOCO97), all the HEMT channels worked but the two SIS channels did not. The problem with the SISs was fixed for the second season (TOCO98). Thus we cover from $l = 60$ to $l = 400$ in multiple frequency bands. In the field we were plagued by refrigerator problems. This resulted in a higher SIS temperature and thus lower sensitivity than we expected from the laboratory measurements.

In this sort of experiment, one must deal with the variable atmospheric temperature and variable local temperature. The data must be edited and one must go to great measures to ensure that the editing does not bias the answer. Of central importance is the correct assessment of the instrument noise. As δT_l^2 is proportional to the measured variance minus the instrument variance, an incorrect assessment of the noise will bias the result (see, for example, [43] and [59] for discussions).

²The Cerro Toco site of the Universidad Católica de Chile was made available through the generosity of Professor Hernán Quintana, Dept. of Astronomy and Astrophysics.

The straight forward way to make sure that the noise is understood is to make combinations of the data in which the sky signal is cancelled out. The analysis of such a null signal should yield the instrument noise. These null combinations should cover multiple time scales and spatial scales. As an example, we show the null tests from the TOCO97 data in Figure 5 (for TOCO98 see [42]). Note that in all cases, the signal is well above the instrument noise and that for each l -space bin, the null tests, regardless of time scale, give consistent noise levels. Additionally, the ratio of the noise between l -space bins can be computed; it agrees with the data. The results from both campaigns are in Table 1. There are roughly 100 more days of 30 and 40 GHz data to analyze.

8. SK/QMAP/TOCO (SQT)

I've tried to come up with an easy-to-state criteria for selecting data sets for a compendium of solid results above $l = 50$. Qualifications for entry onto this list would include confirmation of results, maturity of analyses (of order 30% of the reported data has undergone some sort of reanalysis after publication resulting in significantly different answers), some check for foreground contamination, internally consistent data, and measurements that include internal consistency checks of the data quality and noise levels. I have not been successful. As any caveated selection runs the hazard of being biased toward results that agree with our results, I will use instead a completely subjective criterion. Namely, experiments with which I have been involved over the past few years. The list is given in Table 1.

The SQT data span from 30 to 150 GHz, use different calibrators, involve different analysis packages, different radiometers, different platforms, and different observing strategies.

Except for the QMAP point at $l = 126$ which is somewhat correlated with the other QMAP points, these data can be considered uncorrelated. At low l , all data sets are sample variance limited. The sky coverage varies quite a bit. For SK it is 200 deg², for QMAP 530 deg², for TOCO97 600 deg², and for TOCO98 500 deg².

What is the significance of the down turn from the peak near $l = 200$? The first thing to note is that the D-band data points (TOCO98 in Figure 6) are essentially uncorrelated. There are two data points below the maximum. The net effect is a 5σ detection of a fall from just the TOCO98 data alone. In addition, including the last (low) SK point enhances the probability of a downturn. In other words, from just these data, the down turn is indisputable. and of course there are many other experiments as shown in Figure 1.

In Table 1 we also give the recent analysis of the MSAM data [63]. The

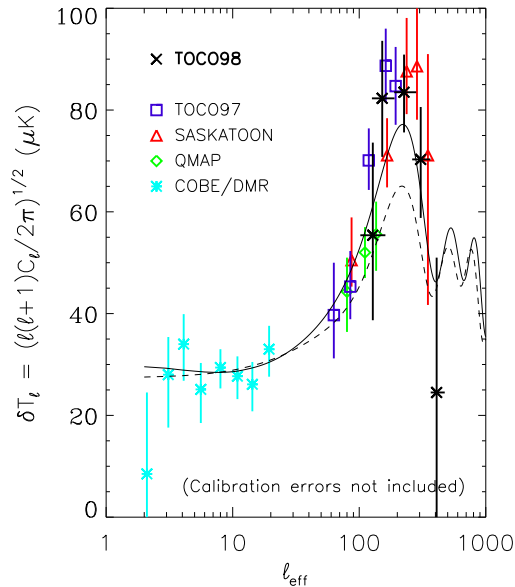


Figure 6. The SK/QMAP/TOCO and COBE/DMR data. For the highest l point, we show the data point using the convention of Knox. The models are the same as in Figure 1. Note that the peak is clearly not at $l = 400$.

MSAM point at $l = 200$ is about 3σ below the mean of the SQT points. Interestingly, the data comprising this point come from a section of sky examined in two MSAM flights [37] and on the ground in the SK experiment [43]. My interpretation is that this is a statistical fluke. MSAM covers only of order 10 deg^2 of sky. The experiments are well enough documented to check this against the MAP data.

9. Finding the peak

Once we have the power spectrum we can either fit the data to models or we can look for nearly model independent parametrizations. Directly fitting to models has been done by a number of groups (e.g. [1], [4], [8], [25], [38], [50], & [58]) In broad brushstrokes, the data are consistent with spatially flat models with a cosmological constant and inconsistent with spatially open models (though this conclusion depends on the selection of data sets [50]). In the following, we give a model independent assessment of the position of the peak.

The richness of the CMB is the very thing that makes it so difficult to fit. In the current stage, one cannot look at the spectrum and get simple

TABLE 1. Selected data. Calibrations errors ($\approx 10\%$) are not included.

Name	l_{eff}	δT_l (μK)	Comments & Reference
TOCO97	63^{+18}_{-18}	$39.7^{+10.3}_{-6.5}$	Torbet et al.
QMAP	80^{+41}_{-41}	$44.3^{+6.7}_{-7.9}$	Foreground subtracted
MSAM	84^{+46}_{-45}	35^{+15}_{-11}	Foreground subtracted
TOCO97	86^{+16}_{-22}	$45.3^{+7.0}_{-6.4}$	Torbet et al.
SK	87^{+39}_{-27}	$50.5^{+8.4}_{-5.2}$	Foreground subtracted
QMAP	111^{+64}_{-64}	$52.0^{+5.0}_{-5.0}$	Foreground subtracted
TOCO97	114^{+20}_{-24}	$70.1^{+6.3}_{-5.8}$	Torbet et al.
QMAP	126^{+54}_{-54}	$55.6^{+6.4}_{-7.2}$	Foreground subtracted
TOCO98	128^{+26}_{-33}	$54.6^{+18.4}_{-16.6}$	Miller et al.
TOCO98	155^{+28}_{-38}	$82.0^{+11.0}_{-11.0}$	Miller et al.
TOCO97	158^{+22}_{-23}	$88.7^{+7.3}_{-7.2}$	Torbet et al.
SK	166^{+30}_{-43}	$71.1^{+7.3}_{-6.3}$	Foreground subtracted
TOCO97	199^{+38}_{-29}	$84.7^{+7.7}_{-7.6}$	Torbet et al.
MSAM	201^{+82}_{-70}	49^{+10}_{-8}	Foreground subtracted
TOCO98	226^{+37}_{-56}	$83.0^{+7.0}_{-8.0}$	Miller et al.
SK	237^{+29}_{-41}	$87.6^{+10.5}_{-8.4}$	Foreground subtracted
SK	286^{+24}_{-36}	$88.6^{+12.6}_{-10.5}$	Foreground subtracted
TOCO98	306^{+44}_{-59}	$70.0^{+10.0}_{-11.0}$	Miller et al.
SK	349^{+44}_{-41}	$71.1^{+19.9}_{-29.4}$	Foreground subtracted
MSAM	407^{+46}_{-123}	47^{+7}_{-6}	Foreground subtracted
TOCO98	409	< 67 (95% <i>conf</i>)	Miller et al

answers. There are multiple sets of parameters that give rise to the same power spectrum if only a certain region of l -space is covered [6]. This degeneracy is broken by including other data sets into the analysis; for instance, one may assume prior knowledge of the Hubble constant or the baryon density.

In an effort to say where the peak is, we have parametrized a generic spectrum by taking the lambda model in Figure 1[61], normalizing it to $\delta T_l = 32$ at $l = 25$ and stretching it in l and changing the amplitude while maintaining the normalization. (To my knowledge, this was done first by Barth Netterfield to the SK data. At that time, we found that the SK peak preferred $h=0.35$, a cosmological constant, or lots of baryons. Basically, anything to make the peak higher than the sCDM peak.) We then compute the likelihood as a function of l and amplitude of the peak. The results are shown in Figure 7 for both the SQT and all the data in Figure 1.

To show what the data prefer, we have done a simple χ^2 analysis assum-

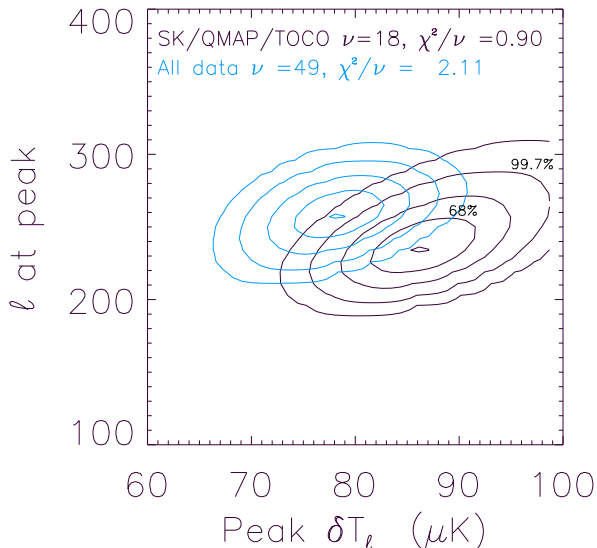


Figure 7. The peak position and amplitude for the SK/QMAP/TOCO data and all the data in Figure 1. DMR was not included. Note that the reduced chi-squared for SQT is completely consistent with statistical uncertainty. Note also that a peak near $l = 400$ is very unlikely. Calibration error shifts the contours left and right.

ing a spatially flat universe and limiting ourselves to variations of Ω_Λ , Ω_b and Ω_{cdm} with $h=0.65$. The SQT data are well described by $\Omega_b = 0.05$, $\Omega_{cdm} = 0.2$, & $\Omega_\Lambda = 0.75$. If one wants to explain the height of the peak without a cosmological constant, then one must have something like $\Omega_b = 0.12$, $\Omega_{cdm} = 0.88$, clearly at variance with a large body of cosmological data.

We have reached the point where there are well developed techniques for measuring and quantifying the anisotropy from balloons and the ground that give reliable and consistent results. This situation will continue to improve with the large interferometers and highly sensitive balloon data coming on line now. The current limitations to the experiments are 1)calibration, 2)sky coverage and 3)knowledge of the beam. The dominant error for the combined SQT data is the calibration. We find that the amplitude of the peak between $l = 150$ and $l = 250$ is $\delta T_l = 82 \pm 3.3 \pm 5.5 \mu K$, the first error is statistical and the second error is from the calibration. A typical intrinsic calibration source accuracy is 5%. Secondly, without full sky coverage, the ultimate error bars cannot be achieved. For instance, if one maps only a quarter the full sky, the error bars will be twice as large as

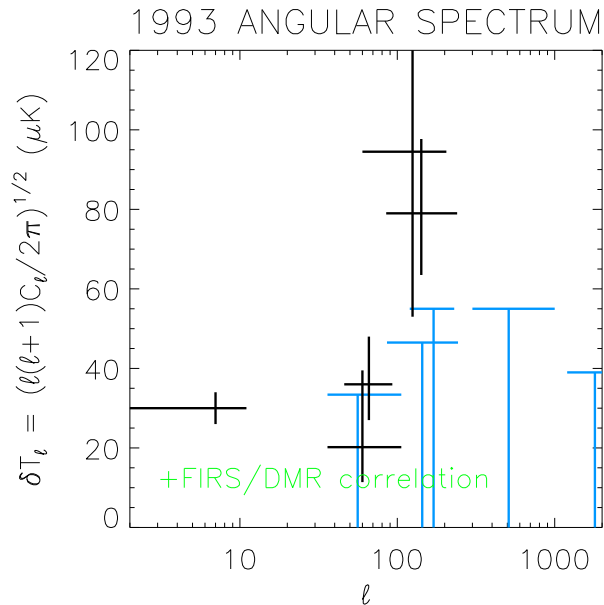


Figure 8. Plot of the CMB angular spectrum of data published in 1993 and before. The upper limits are all at 95% confidence. No measurement between $l = 100$ and $l = 1000$ has been confirmed.

potentially achievable. Finally, there is no reason that the beams cannot be known to high accuracy. The problem is that they must be measured *in situ* and these measurements can be difficult. To the accuracy needed, beams can no longer simply be modeled by two dimensional Gaussian profiles.

10. The past

It is amusing to look back and see how far we have come in the past six years. Figure 8, is a plot of all the data that were published in or before 1993 with sensitivities at an interesting level. I've converted the reported limits on the Gaussian autocorrelation function to the modern band powers using [5] and [30]. The full power spectrum of DMR had not been published at this time. Based on these data, one would be surprised by the models that currently fit so well.

There have been tremendous advances on the theoretical front as well. Model predictions have been brought to the masses through CMBFAST [52]; textures and similar mechanisms are generally believed to be inconsistent with the current data [45], and there are many classes of isocurvature models that are no longer viable. As the theories improve, some of these

models may arise again or we may find that the anisotropy is an admixture of adiabatic, isocurvature, and texture perturbations.

11. The future

At $l < 1000$ the future is in multielement interferometers [11] [16], long duration balloon flights e.g ([10]), and satellite missions. At $l < 20$, the sky can only be mapped precisely from a satellite. For $l > 1000$, measurements can be made from the ground. Arrays of bolometers and interferometers seem ideal. The polarization has yet to be detected but experiments coming on line now should be able to do the job within a year or so.

There are now four space missions on the books. There is NASA's MAP satellite which just had its Launch-1 year review, there is ESA's Planck satellite (with collaborative NASA support) which is scheduled for a 2007 launch, there is the SPORT mission which plans to measure the polarization of the CMB at HEMT frequencies from the space station [14], and, in NASA's technological road map, there is a mission, CMBPOL, to measure the polarization of the CMB in ≈ 2015 . The later is in the talking phase [46]. I shall focus on MAP and Anthony Lasenby will focus on Planck.

12. MAP

The primary goal of MAP³ is to produce a high fidelity, polarization sensitive, full sky map of the cosmic microwave background anisotropy. From its inception, the focus has been on how one makes a full sky map with negligible systematic error. MAP is a MIDEX mission which means there is minimal redundancy as well as firm cost and schedule caps. MAP was proposed in June 1995, selected in April 1996, and is planned for a November 2000 launch. It was also proposed with the notion of getting the data to the community as fast as possible. We plan to make maps public nine months after we scan the whole sky (roughly one year after getting to L2).

Sources of systematic error in mapmaking include "1/f noise" (any variations from tenths of seconds to minutes) in the detectors and instrument, magnetic fields, and sidelobe contamination. Our systematic error budget allows for a total of $5 \mu\text{K}$ of extraneous signal *before* any modeling of the source of the contamination. The $5 \mu\text{K}$ applies to all angular scales and time scales though the most troublesome sources are the ones that are synchronous with the spin period.

³MAP is a collaboration between NASA (Chuck Bennett [PI], Gary Hinshaw, Al Kogut, & Ed Wollack), Princeton (Norm Jarosik, Michele Limon, Lyman Page, David Spergel & David Wilkinson), Chicago (Steve Meyer), UCLA (Ned Wright), UBC (Mark Halpern), and Brown (Greg Tucker)

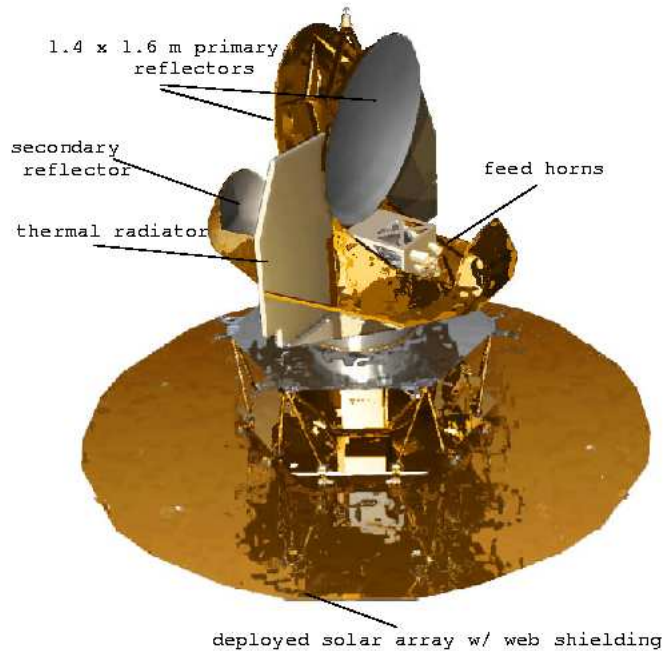


Figure 9. Picture of MAP with the solar arrays deployed. The receivers are located directly beneath the primary mirrors and are cooled by the thermal radiators. The Earth, Moon, and Sun are beneath the solar arrays.

MAP is being documented on the web as the instrument is built and tested. Official information may be obtained at <http://map.gsfc.nasa.gov/>; technical papers are in preparation.

12.1. MISSION OUTLINE

The design guidelines for MAP were:

- **Simplicity** Other than the thruster valves and attitude control reaction wheels, there are no moving parts when the satellite is at L2. For taking science data, there is only one mode of operation. MAP is passively cooled to ≈ 95 K.
- **Stability** The orbit at the Earth-Sun Lagrange point, L2, is thermally stable and has a negligible magnetic field. L2 is roughly 1.5×10^6 km from Earth and the Sun, Earth, and Moon are always “under” the spacecraft. (It will take approximately 3 months to get to L2.)

- **Heritage** No major new components were required except the NRAO W-band amplifiers. These were designed for MAP.
- **Ease of Integration** The mission relies on the complete understanding of the systematic noise levels. The magnitude of many of the systematic effects are easily determined when the instrument is warm.

with spacecraft and mission parameters as follows:

- **Mission Duration** Two years at L2. It can last longer.
- **Mass** 800 kg
- **Power** 400 W
- **Launch Vehicle** Delta 7425 (4 strap on motors).

12.2. RECEIVERS

MAP uses pseudo-correlation radiometers to continuously measure the difference in power from two input feeds on opposite sides of the spacecraft. The detecting elements are HEMTs designed by Marian Pospieszalski at the National Radio Astronomy Observatory (NRAO). The wide bandwidth and high sensitivity of the HEMTs, even while operating near 95 K, are what make MAP possible. There are ten feeds on each side of the spacecraft and each feed supports two polarizations, thus there are a total of twenty differential chains. Each receiver chain uses four amplifiers (two at ≈ 95 K and two at ≈ 290 K) for a total of eighty amplifiers. The radiometers are configured so that they difference two polarizations whose electric fields are parallel.

The key characteristic of the receivers is their low $1/f$ noise. The noise level at the spin rate, 8 mHz, is virtually the same as at the 2.5 kHz switching rate. This means that the receivers will not correlate noise from one pixel to the next. To put this receiver performance in perspective, we note that the $1/f$ knee of the W-band HEMTs alone is near 1 kHz. There is a complete model of the receivers from the feeds to the detector outputs, including all the support electronics. With the model, and measurements that correlate the model to reality, we determine the sensitivity of the output to temperature variations in each component. The temperatures of the most sensitive components are monitored during flight to roughly 1 mK accuracy.

Due to the wide HEMT bandwidth, the central effective frequency of the band depends on the source one is observing. Between dust and synchrotron sources, the shift is greater than 1 GHz in W-band. This will have to be taken into account when observing different sources. Below is a table of the representative central frequencies and noise bandwidths of the receivers. The values in flight will be different and are channel dependent.

TABLE 2. MAP band centers and noise bandwidth

Band	f_c (GHz)	Bandwidth (GHz)	# Channels
K	23	5.3	4
K _a	33	7	4
Q	41	8.4	8
V	61	12	8
W	95	17	16

12.3. OPTICS

The optics comprises two back-to-back telescopes. The secondary of each telescope is illuminated by a cooled corrugated feed which is the input to the receiver chain. The reflector surfaces are shaped to optimize the beam profiles but to a good approximation, the telescopes are Gregorian. The Gregorian design was chosen because it is more compact than the Cassegrain and because it could accommodate the back-to-back feed geometry required for the radiometers. We considered a wide variety of designs, including single and triple reflector systems, but the Gregorian suited our needs best.

The feeds and receivers occupy a large space. As a consequence the beam profiles are not symmetric (see Table 3). The scan strategy, to a first approximation, symmetrizes the beam profile. Thus even if the beams were 2-D Gaussians to start with, the symmetrized profile would not be Gaussian. Likewise, the window functions are not simply Gaussian. Nonetheless, the beam profiles and windows can be parametrized by Gaussians for most work. The data in the table are representative, the final beams will be measured in flight with sub-percent accuracy.

TABLE 3. Approximate E & H plane beam θ_{FWHM}

Band	θ_E (deg)	θ_H (deg)
K	0.95	0.75
K _a	0.7	0.6
Q	0.45	0.5
V	0.3	0.35
W	0.21	0.21

Outside of making the optics fit into the MIDEX fairing, one wants to ensure that one measures power from only the main beam. The Sun, Earth, and Moon, which are always at least 100° away from the main beam, are blocked by the solar arrays. The contribution from these sources is computed to be much less than $1\mu\text{K}$. The more difficult source to block is the Galaxy which illuminates the feeds from just over the top of the secondary. To block it, we substantially oversized the secondary, so that at its edge the illumination from the feed is less than 10^{-5} the illumination at the center (< -50 dB edge taper).

The optics are modeled using a program from YRS Associates[66] that solves for the currents on the reflectors as waves propagate through the system. The measured beam profiles (all have been measured at ten frequencies across the band) are in excellent agreement with the predictions. Chris Barnes modified the code to run on a supercomputer so that we can also predict the sidelobes. The sidelobe measurements agree well with the predictions.

Using the models, we can estimate the contribution to MAP from the Galaxy. Our model includes a spinning dust component so that the frequency spectrum resembles something like that shown in [26]. We then fly MAP over the Galaxy and record two signals. One signal is the rms difference between the two telescopes with the response integrated over the whole sky; the second signal is the same except with the contribution from the main beams subtracted. In other words, the second method tells how much Galactic signal comes through the sidelobes or from angles greater than $\approx 4^\circ$ from the main beam. We do this for $|b| > 15$. The model is only approximate and does not yet include a contribution from extragalactic sources. Of course, the model will be updated after we measure what the Galaxy is really like.

TABLE 4. Approximate Galactic contributions for $|b| > 15^\circ$

Band	Galactic contribution (μK)	Sidelobe contribution (μK)
K	120	16
K _a	60	2
Q	40	4
V	20	0.2
W

To put these numbers in perspective, the *rms* magnitude of the CMB is about $120\mu\text{K}$. In K band, the *rms* Galaxy signal is roughly the same. To first order, these add in quadrature to produce a signal with an *rms* of

170 μK . In V-band, the galactic contribution is far less; it will change the power spectrum by $\approx 2\%$ if uncorrected. These rough numbers show that the power spectrum estimates are quite robust to the Galactic contamination.

As we have emphasized, the goal of MAP is to make maps; the power spectrum is just one way to quantify them. In producing a map of the CMB, we will clearly have to model and subtract the Galaxy. The rightmost column in Table 4 gives an indication of the contribution to the map if the sidelobe contribution is not accounted for.

12.4. SCAN STRATEGY

The scan strategy is at the core of MAP and can only be realized at a place like L2. To make maps that are equally sensitive to large and small scale structure, large angular separations must be measured with small beams. To guard against variations in the instrument, as many angular scales as possible should be covered in as short a time as possible. MAP spins and precesses like a top. There are four time scales. The beams are differenced at 2.5 kHz; the satellite spins at 0.45 rpm; the spin axis precesses around a 22.5° half angle cone every hour; and the sky is fully covered in six months. In one hour, roughly 30% of the sky is mapped.

As of this writing, the core of a pipeline exists to go from the time ordered data to maps to a power spectrum.

12.5. SCIENCE

Of primary interest, initially, will be the angular spectrum. It will be calibrated to percent accuracy and there will be numerous independent internal consistency checks. Of central importance will be the accompanying systematic error budget. The power spectrum will be sample variance limited up to $l \approx 700$. In other words, if the systematic errors and foreground contributions are under control, it will not be possible to determine the angular spectrum any better. MAP will be sensitive up to $l \approx 1000$.

The angular spectrum is not the best metric for assessing MAP. The primary goal is a map with negligible correlations between pixels. With such a map, analyses are simplified and the map is indeed a true picture of the sky. MAP should be able to measure the temperature-polarization cross correlation [15] and will be sensitive to the polarization signal itself. Correlations with X-ray maps will shed light on the extended Sunyaev Zel'dovich effect (not to mention the dozen or so discrete sources[51]). Correlations with the Sloan Digital Sky Survey will inform us about large scale structure. MAP will be calibrated on the CMB dipole and thus will be able to calibrate

radio sources and planets to a universal system. It will also help elucidate the emission properties of the intergalactic medium.

13. Conclusions

This is a truly amazing era for cosmology. Our theoretical knowledge has advanced to the point at which definite and testable predictions of cosmological models can be made. For the CMB anisotropy, results from the angular power spectrum, frequency spectrum, statistical distribution, and polarization must all be consistent. In addition, these results must be consistent with the distribution, velocity flows, and masses of galaxies and clusters of galaxies as well as the age of the universe. There is a fantastic interconnecting web of constraints.

Using the CMB to probe cosmology is still in its early phase. After all, the anisotropy was discovered less than a decade ago. As cosmological models and measurements improve, the CMB and other measures will become a tool for probing high energy physics. For example, should the cosmological constant survive, we will have a handle on new physics in the early universe that we could never have obtained from accelerators.

14. Acknowledgements

I thank Chuck Bennett, Mark Devlin, Amber Miller, Suzanne Staggs, and Ned Wright for comments that improved this article. In the course of writing, a paper describing the VIPER experiment[47] appeared. These data are not included in the analysis nor do they change any conclusions.

References

1. Bahcall, N., Ostriker, J. P., Perlmutter, S., and Steinhardt, P. J., 1999, *Science*, 284, 1481-1488 (astro-ph/9906463)
2. Baker, J.C., Grainge, K., Hobson, M.P., Jones, M.E., Kneissl, R., Lasenby, A.N., O'Sullivan, C.M.M., Pooley, G. Rocha, G., Saunders, R., Scott, P.F., Waldram, E.M. 1999, Submitted to MNRAS, astro-ph/9904415
3. Barreiro, R. B., astro-ph/9907094
4. Bartlett, J. G., Blanchard, A. Douspis, M. Le Dour, M., Proc Evol of Large Scale Structure, garching, Aug 1998. astro-ph/9810318
5. Bond, J. R., *Astro. Lett. & Comm.* Vol 32, No. 1, 1995. Presented in 1994.
6. Bond, J. R., Crittenden, R., Davis, R. L, Efstathiou, G., & Steinhardt, P. J. 1994, *Phys Rev Letters*, 72, 1, pg 13
7. Bond, J. R., Efstathiou, G., Tegmark, M. 1998, *MNRAS*, 50, L33-41
8. Bond, J. R., Jaffe, A. H., *Phil Trans R. Soc. Lond.* astro-ph/9809043
9. Bond, J. R., Jaffe, A. H., Knox, L. 1999, Accepted in *Ap.J.*, astro-ph/9808264
10. BOOMERanG at the web sites <http://phobos.caltech.edu/~lgg/boom/boom.html> or <http://www.phys.uniroma1.it/DOCS/RESEARCH-98/ACS/8-BOOMERANG-deBernardis.html>
11. Cosmic Background Imager web site <http://astro.caltech.edu/~tjp/CBI/>

12. Coble, K., et al. 1999, astro-ph/9902195
13. Coble, K. Ph.D. Thesis, Univ. of Chicago, 1999.
14. Cortiglioni et al. astro-ph/9901362.
15. Crittenden, R. G., Coulson, D. & Turok, N. Phys Rev D, 1995, D52, 5402. See also astro-ph/9408001 and astro-ph/9406046
16. Degree Angular Scale Interferometer web site <http://astro.uchicago.edu/dasi/>
17. Davies, R.D., & Wilkinson, A. in "Microwave Foregrounds" APS Conference Series, pg. 77, Vol 181, 1999, A. de Oliveira-Costa & M. Tegmark eds.
18. Dicker et al. astro-ph/9907118. Submitted to MNRAS 1999.
19. de Oliveira-Costa, A., Kogut, A., Devlin, M. J., Netterfield, C. B., Page, L. A., Wollack, E. J. 1997 Ap.J. Letters, 482, L17-L20
20. de Oliveira-Costa, A., Devlin, M. J., Herbig, T. H., Miller, A.D., Netterfield, C. B., Page, L. A. & Tegmark, M. 1998 Ap.J. Letters, 509, L77
21. de Oliveira-Costa, A., Tegmark, M., Page, L.A., Boughan, S. 1998 Ap.J. Letters, 509, L9
22. de Oliveira-Costa, A. 1999. Private communication and work in progress. See related maps at <http://www.sns.ias.edu/~angelica/skymap.html>.
23. de Oliveira-Costa, A. 1999. Private communication. Work in progress on foreground subtraction for QMAP data.
24. Devlin, M. J., de Oliveira-Costa, A., Herbig, T., Miller, A. D., Netterfield, C. B., Page, L. A., & Tegmark, M. 1998, ApJ Letters, 509, L73
25. Dodelson, S. & Knox, L., 1999, astro-ph/9909454.
26. Drain, B. T. & Lazarian, A. 1999, astro-ph/9902356, in *Microwave Foregrounds*, ed A. de Oliveira-Costa & M. Tegmark APS Conference Series, Vol 181, pg 133, (ASP:San Francisco)
27. Fixsen, D. J., et al. 1997 (astro-ph/9704176)
28. Ganga, K. M. et al. 1993, Ap.J. 432:L15-L18.
29. Glanz, J. 1999. In the "News" section, Science, Vol 283. See also the VIPER web site at <http://cmbr.phys.cmu.edu>
30. Gundersen, 1999, Ph.D. Thesis from U.C. Santa Barbara, 1995
31. Gush, H., Halpern, M., & Wishnow, E. H., 1990, Phys. Rev. Letters, 65, 537
32. Halpern, M., & Scott, D. in *Microwave Foregrounds*, ed A. de Oliveira-Costa & M. Tegmark APS Conference Series, Vol 181, pg 283, (ASP:San Francisco)
33. Herbig, T., Devlin, M. J., de Oliveira-Costa, A., Miller, A. D., Page, L. A., & Tegmark, M. 1998, Ap.J. Letters, 509, L73
34. Hu, W. and White, M. 1996, Ap.J. 471:30 This is also available through <http://www.sns.ias.edu/~whu>
35. Huey, G. & Steinhardt, P., 1999, The updated cosmic triangle available through <http://feynman.princeton.edu/~steinh/>
36. Kerr, A. R., Pan, S. -K., Lichtenberger, A. W., and Lloyd, F. L. 1993, Proceedings of the Fourth International Symposium on Space Terahertz Technology, pp 1-10
37. Knox, L., Bond, J. R., Jaffe A. H., Segal, M. & Charbonneau, D. Phys.Rev. D58 (1998) 083004, astro-ph/9803272.
38. Lineweaver, C. H., Science, 284, 1503-1507, 1999. See also astro-ph/9909301.
39. Mather, J. C., et al. 1990, Ap.J. Letters, 354:L37.
40. Mather, J. C., et al. 1999, Ap.J., 512. See also astro-ph/9810373 and Fixsen, D. J., et al. 1996, Ap.J., 473:576. (astro-ph/9605054)
41. MAXIMA's web site <http://cfpa.berkeley.edu/group/cmb/gen.html> contains more information.
42. Miller, A. D., Devlin, M. J., Dorwart, W. Herbig, T., Nolta, Page, L., Puchalla, J., Torbet, E., & Tran, H. 1999, Ap.J. Letters, 524, L1-4.
43. Netterfield, C. B., Devlin, M. J., Jarosik, N., Page, L., & Wollack, E. J. 1997, Ap.J. 474, 47
44. Generation of Large Scale Structure ed D.N. Schramm and P. Galeotti (Kluwer, Netherlands), p75.

45. Pen, U., Seljak, U., & Turok, N. 1997, Phys Rev Letters, 79:1611
46. Peterson, J.B. et al. astro-ph/9907276
47. Peterson, J.B. et al. astro-ph/9910503
48. Pospieszalski, M. W. 1992, Proc. IEEE Microwave Theory Tech., MTT-3 1369; and Pospieszalski, M. W. 1997, Microwave Background Anisotropies, ed F. R. Bouchet (Gif-sur-Yvette: Editions Frontières): 23-30
49. Pospieszalski, M. W. et al. 1994 IEEE MTT-S Digest 1345
50. Ratra, B., *et al.* 1999 Ap.J. 517:549
51. Refregier, A., Spergel, D. & Herbig, T. Ap.J, 1998, astro-ph/9806349
52. Seljak, U. and Zaldarriaga, M. 1998. The CMBFAST code is available through <http://www.sns.ias.edu/matiasz/CMBFAST/cmbfast.html>. See also 1996 Ap.J. 469, 437-444
53. Smoot, G.F., *et al.* 1992, Ap.J. Letters 396, L1
54. Staggs, S. T., et al, 1996. Ap.J. Letters, 473, L1
55. Tegmark, M. 1997, PRD, 55, 5895
56. Tegmark, M., de Oliveira-Costa, A., Devlin, M., Netterfield, C.B., Page, L. & Wollack, E. 1997, Ap.J. Letters, 474:L77
57. Tegmark, M., Eisenstein, D., Hu, W., & de Oliveira-Costa, A. 1999, Submitted to Ap.J., astro-ph/9905257
58. Tegmark, M., 1999, Ap.J. 514, L69-L72. See also astro-ph/9809201
59. Torbet, E., Devlin, M. J., Dorwart, W. Herbig, T., Nolte, Miller, A. D., Page, L., Puchalla, J., & Tran, H. 1999, ApJ Letters, astro-ph/9905100, 521, L79
60. Turner, M.S., 1999, astro-ph/9904051
61. Wang, L., Caldwell, R.R., Ostriker, J. P. & Steinhardt, P.J. 1999, astro-ph/9901388
62. White, M., & Bunn, E. 1995, Ap.J. Letters 443:L53
63. Wilson, G. W., et al. 1999, Submitted to Ap.J., astro-ph/9902047
64. Wollack, E. J., Devlin, M. J., Jarosik, N.J., Netterfield, C. B., Page, L., Wilkinson, D. 1997, Ap.J., 476, 440-447
65. Wright E. IAS CMB Data Analysis Workshop. astro-ph/9612006.
66. Rahmat-Samii, Y., Imbriale, W., & Galindo, V. YRS Associates, 4509 Tobias Ave. Sherman Oaks, CA 91403